

Behavior of URu₂Si₂ in an applied magnetic field

P. Santini

Institute of Theoretical Physics, University of Lausanne, CH-1015 Lausanne, Switzerland

(Received 11 September 1997; revised manuscript received 1 December 1997)

Electrical resistivity, thermal expansion, and magnetization of URu₂Si₂ in an applied magnetic field are analyzed within a model based on quadrupolar ordering of U ions with localized *f* electrons. This model, which had been shown to be consistent with macroscopic properties in a field tending to zero, can be used to account for the observed behavior in a finite field. [S0163-1829(98)02610-1]

I. INTRODUCTION

Actinide compounds possess extremely rich and complex physical properties, many of which result from *f* electrons being close to the localization-delocalization transition. It is usually difficult to determine on which side of this transition each compound is located. While direct measurements of the volume and topology of the Fermi surface and their comparison with band calculations may sometimes be decisive, most physical properties are often compatible with both localization or itineracy. For instance, an enhanced specific heat coefficient may be due to the formation of heavy quasiparticle bands, but also to various effects not related to itineracy,¹ including the formation of a single-ion-type Kondo resonance² or the effect of local moment fluctuations on non-*f* conduction electrons.³ Sharp crystal-field excitations revealed by inelastic neutron scattering (INS) are a sufficient but not necessary condition for localization, since even in insulating compounds with unambiguously localized *f* electrons, such as NpO₂, crystal-field excitations may be unexpectedly broad.⁴ In USb, a model based on localized *f* electrons in a crystal-field gives excellent results⁵ in spite of the fact that crystal field excitations are so broad as to be undetectable by inelastic neutron scattering.⁶

The properties of URu₂Si₂ are exemplary of this ambiguity. De Haas-van Alphen measurements of the Fermi surface properties are not conclusive,⁷ while the Fermi-surface topology measured by positron annihilation techniques⁸ disagrees with that calculated by assuming itinerant *f* electrons. The compound displays a characteristic temperature scale T_M of about 50 K (see Ref. 9 and references therein), which is sometimes attributed to a loosely characterized heavy-fermion state developing below T_M . However, the macroscopic behavior is certainly not prototypical of such a state, while it is reminiscent of that of localized *f*-electron compounds with a singlet crystal electric field (CEF) ground state. For instance, in PrNi₅ a temperature scale of about 20 K characterizes macroscopic properties such as susceptibility, resistivity, specific heat,¹⁰ and thermal expansion¹¹ in a similar way as in URu₂Si₂, and is related to the energy of the first excited CEF state. Indeed, it was shown in Ref. 9 that a satisfactory interpretation of the behavior of URu₂Si₂ may be given by a localized *f*-electron model, where $k_B T_M$ is identified with a CEF energy gap.

At $T_N = 17.5$ K the compound undergoes a phase transi-

tion, marked by strong anomalies in macroscopic observables. Below T_N , *f*-electron localization is evidenced by sharp excitations observed in INS, while above T_N excitations are broad.¹²

The strong increase of T_N as a function of an applied pressure (it reaches 35 K with a pressure of 80 Kbar) (Ref. 13) suggests the phase transition to involve local degrees of freedom of the U ions rather than itinerant electrons. Also, in Doniach's picture¹⁴ of the magnetism of Kondo-lattice compounds as resulting from the competition between interion interactions and Kondo-type fluctuations, URu₂Si₂ would be located on the extreme left-hand side of the phase diagram, where Kondo fluctuations are negligible.

The transition has been attributed to a type-I antiferromagnetic (AFM) ordering along the *c* axis, with an ordered moment $\mu \sim 0.03 \mu_B$ at saturation.^{12,15} However, the correlation length is finite and sample dependent,¹⁶ so that the order is not truly long ranged. No way has been found so far to reconcile the tiny value of the moment with the large macroscopic anomalies observed at T_N . Moreover, the sample dependence of the $\mu(T)$ curve¹⁶ contrasts with macroscopic anomalies occurring always sharply at T_N .

The only way to overcome these difficulties is to admit that macroscopic anomalies are not associated with μ , but rather with a hidden order parameter (OP) not yet observed directly in elastic-scattering experiments. Various ideas have been put forward.¹⁷⁻¹⁹ In Ref. 9 it was shown that by identifying this OP with one of the electric quadrupoles $Q = Q_{xy}$ or $Q = Q_{x^2-y^2}$, the value of T_N , the anomalies in the linear and nonlinear susceptibilities, the gap and the oscillator strength measured in inelastic scattering, and the value of the entropy at T_N are reproduced at a semiquantitative level. Recently, point-contact experiments have also been shown to agree with this model.²⁰ The fact that, below T_N , no orthorhombic macroscopic distortion either of *xy* or $x^2 - y^2$ symmetry takes place²¹ rules out ferroquadrupolar order. On the other hand, the weak, but highly uncommon softening of the ($c_{11} - c_{12}$) elastic constant below 70 K (Ref. 21) is an indication (but not a proof) that antiferroquadrupolar order may take place.

The opposite behavior of μ and Q with respect to time reversal implies that two accidentally close, but distinct, phase transitions exist.²² In view of the smallness of μ , the macroscopic anomalies originate entirely from the quadrupolar ordering. For instance, in UPt₃ a tiny moment state very

similar to that of URu_2Si_2 is observed by neutron scattering, but no macroscopic signs of this state are seen. On the other hand, of these two transitions only the magnetic one may be seen easily in neutron-diffraction experiments, since neutrons do not couple directly with electric quadrupoles. Although an antiferroquadrupolar order may produce local lattice distortions, such distortions may be too small to be detected. For instance, in CeB_6 the antiferroquadrupolar state is not directly detected by neutron diffraction, while it can be detected indirectly by diffraction in an applied magnetic field.²³ In fact, the magnetic moments induced by the field display a modulation reflecting that of the electric quadrupolar moments of Ce ions. Similarly, when a field is applied in the ab plane of URu_2Si_2 , the induced moments should possess a modulation if the order is antiferroquadrupolar. More precisely, a modulation is obtained by applying the field along the a or b axes if it is $Q_{x^2-y^2}$ which orders, and by applying the field along the diagonals of the two-dimensional cell if it is Q_{xy} which orders. However, since the magnetic susceptibility to a field applied in the basal plane is very low, detecting the modulation by diffraction would require a field much stronger than that used for CeB_6 (~ 7 T).

That a quadrupolar and a magnetic phase transition have similar transition temperatures is not unusual, since in actinide and in some rare-earth compounds one does not expect the interion multipolar couplings to decrease with increasing multipole rank. This is the case when such couplings originate mainly from virtual phonon or virtual hybridization processes. Examples exist of compounds possessing a double quadrupolar-magnetic transition with transition temperatures of the same order (see Ref. 24 for a review), such as CeB_6 , with transition temperatures of $T_1=3.2$ K (antiferroquadrupolar) and $T_2=2.4$ K (antiferromagnetic); CeAg , with $T_1=15.9$ K (ferroquadrupolar) and $T_2=5.2$ K (ferromagnetic); TmZn , with $T_1=8.55$ K (ferroquadrupolar) and $T_2=8.12$ K (ferromagnetic); TmGa_3 , with $T_1=4.29$ K (antiferroquadrupolar) and $T_2=4.26$ K (antiferromagnetic); and UPd_3 , with $T_1=7$ K (antiferroquadrupolar) and $T_2=5$ K (antiferromagnetic). In this latter the magnetic moment is even smaller than in URu_2Si_2 . Even in an insulating compound, such as UO_2 , the quadrupole coupling via virtual phonon exchange is as large as the magnetic exchange, of the order of 40 K.²⁵ Of course, the pure electrostatic interaction between quadrupoles is much smaller, of the order of 1 K, but it is not the relevant interaction mechanism.

The existence of two different phase transitions in URu_2Si_2 is demonstrated by the difference in behavior of μ and of the macroscopic anomalies when a magnetic field is applied along the c axis. While T_N as deduced from these anomalies reduces to zero at a field of about 40 T (in correspondence with metamagnetic transitions), μ seems to disappear around 14 T.^{26,27}

In this paper, the model developed in Ref. 9 is analyzed with a finite magnetic field H applied along c , and shown to be consistent with experiment. The magnetic (linear and non-linear) response to a field tending to zero has already been considered in Ref. 9.

II. MODEL AND RESULTS

The mean-field (MF) Hamiltonian is

$$\mathcal{H} = \sum_{k,q} B_k^q O_k^q - \lambda Q \langle Q \rangle - g \mu_B J_z H, \quad (1)$$

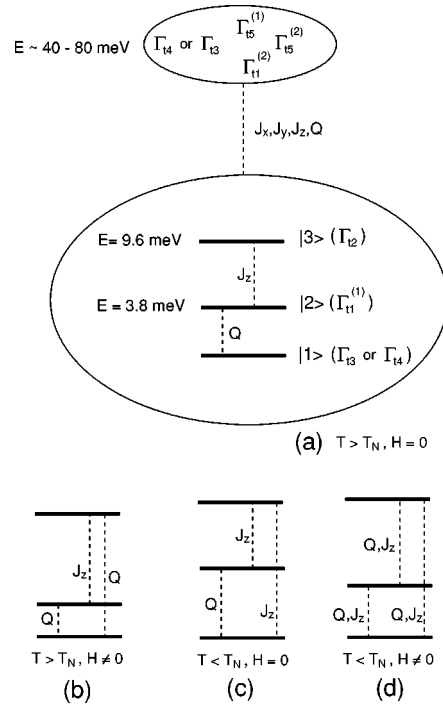


FIG. 1. Qualitative picture of the energy spectrum for various temperatures and fields. Only the three low-lying levels are reproduced in (b), (c), and (d). Dashed vertical lines represent nonzero matrix elements for J_x , J_y , J_z , and Q , with $Q=Q_{x^2-y^2}$ or $Q=Q_{xy}$ depending on whether the ground singlet has Γ_{13} or Γ_{14} symmetry, respectively. The explicit form of the states is given in Ref. 9.

where $O_k^q [(k,q)=(2,0),(4,0),(4,4),(6,0),(6,4)]$ are Stevens operator equivalents for $J=4$, and B_k^q are the CEF parameters. $Q=J_x^2-J_y^2$ or $Q=J_x J_y+J_y J_x$ depending on whether the OP has Γ_{13} or Γ_{14} symmetry, respectively. $\langle Q \rangle$ is the self-consistent mean value of Q (the OP),²⁸ λ is the MF constant, and $g=0.8$.

The tiny moment AFM state is disregarded, since it is expected to give negligible macroscopic effects. Moreover, we think that this unusual state is not contained in MF models analogous to Eq. (1), and is lost in some of the many approximations one implicitly makes to use these models, such as neglecting disorder, short-range correlations, or small charge fluctuations in the $5f$ shell (these latter were considered in Ref. 19).

The determination of the parameters and the corresponding CEF spectrum are described in Ref. 9. We recall (see Fig. 1) that there are three CEF singlets ($|1\rangle$, $|2\rangle$, and $|3\rangle$) at low energy belonging to representations Γ_Q , Γ_{11} , and Γ_{12} (Γ_Q is the representation to which the OP belongs, either Γ_{13} or Γ_{14}), with gaps $\Delta_{12}\sim 3.8$ meV and $\Delta_{13}\sim 9.6$ meV in the paramagnetic phase and with zero applied field. The above-mentioned energy scale $k_B T_M$ is identified with Δ_{12} . While Q connects $|1\rangle$ and $|2\rangle$, J_z connects $|2\rangle$ and $|3\rangle$. Below T_N , and with $H=0$, $|1\rangle$ and $|2\rangle$ are mixed by the molecular field $\lambda \langle Q \rangle$, and J_z connects the ground state with $|3\rangle$, too, with a strength dependent on λ . Identifying $\langle 1|J_z|3\rangle$ with the matrix element probed by INS led to choosing $\lambda\sim 0.185$ meV.

Note that the two possible Q operators coincide with the O_2^2 and O_2^{-2} Stevens operator equivalents of the CEF literature. Thus the term $\lambda Q \langle Q \rangle$ may be seen as a local ortho-

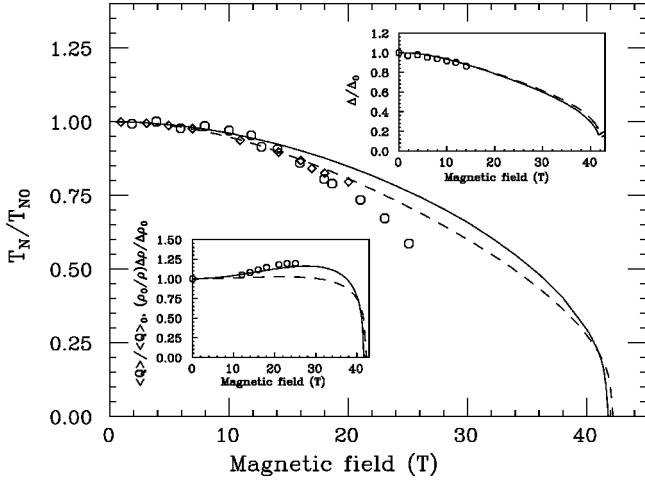


FIG. 2. Transition temperature vs field from Eq. (1). Upper inset: gap $\Delta \equiv \Delta_{12}$ vs field at $T=0$ from Eq. (1). Lower inset: order parameter vs field at $T=0$ from Eq. (1), and measured height of the anomaly in resistivity ρ for field and current along the c axis, divided by $\rho(T_N(H))$. Circles and diamonds: experimental values from Refs. 26 and 27, respectively. Dashed curves: $\lambda=0.185$ meV (giving $T_{N0}=22$ K, $\Delta_0=6.6$ meV, and $\langle Q \rangle_0=5.1$). Full curves: $\lambda=0.175$ meV (giving $T_{N0}=17.5$ K, $\Delta_0=5.2$ meV, and $\langle Q \rangle_0=3.76$). Experimentally, $\Delta_0=4.4$ meV. Subscript 0 refers to $H=0$.

rhombic CEF with an effective CEF parameter $\lambda \langle Q \rangle$. The two effective single-ion Hamiltonians \mathcal{H}_A and \mathcal{H}_B corresponding to the two possible symmetries of the OP are related to each other by a rotation of $\pi/4$ about the c axis, $\mathcal{H}_A = \exp(iJ_z \pi/4) \mathcal{H}_B \exp(-iJ_z \pi/4)$.

A. Transition temperature

When the field H increases, $|2\rangle$ and $|3\rangle$ mix and repel, and eventually Δ_{12} vanishes and a crossing (below T_N an anticrossing) of levels occurs. In the paramagnetic phase, H changes the single-ion quadrupolar susceptibility χ_Q conjugated to the OP by decreasing Δ_{12} , with $|\langle 1|Q|2\rangle|$ remaining approximately constant (this would lead to an increase of χ_Q and T_N) and by decreasing the contribution to χ_Q coming from the coupling with high-lying CEF states. The net result, not obvious *a priori*, is a monotonic decrease of T_N , which, within model (1), is related to χ_Q by the relation $\chi_Q(T_N) = \lambda^{-1}$. The calculated $T_N(H)$ shown in Fig. 2 correlates well with experiment, and reduces to zero around 40 T, a value consistent with that extrapolated from experimental data.^{26,27} In addition to the model of Ref. 9, for which $\lambda=0.185$ meV gives $T_N(0)=22$ K, we also consider the same model with $\lambda=0.175$ meV which, giving the right $T_N(0)=17.5$ K, makes comparison with experiments easier, although it compares somewhat worse with INS. $T_N(H)$ is seen to be similar in both cases.

B. Resistivity

Within this model, a major source of resistivity ρ is found in scattering processes of conduction electrons due to crystal field excitons and to thermal fluctuations of the U multipolar moments.²⁹ Processes involving J_z (the usual spin disorder scattering), Q , and $O_2^0 = 3J_z^2 - J(J+1)$ (electric quadrupole disorder scattering) are expected to be relevant.²⁹ A full cal-

ulation of the resistivity would require fixing too many parameters to be meaningful. Even by making unrealistic approximations for conduction electrons, such as assuming one spherical band, one should fix the value of the three (possibly field-dependent) coupling constants of conduction electrons with the mentioned U moments. Moreover, there is a coupling between dipoles and quadrupoles on different ions which makes the excitations dispersive, i.e., not purely CEF-like. Because of these complications we prefer to consider only those properties of the resistivity which we expect not to depend on details. These are the field-dependent energy scale of the inelastic excitations which scatter conduction electrons below T_N , the sign of the magnetoresistivity above T_N , and the field dependence of the jump in the resistivity at T_N .

At zero or small applied field below T_N the spectral weight of magnetic excitations concentrates at energies of the order of 6–13 meV.¹² This energy scale is set by Δ_{13} within the present model [see Fig. 1(c)], with the width of the observed spectral weight being due to dispersion. On the other hand, since the energy scale of quadrupole excitations is lower, being set by Δ_{12} , quadrupole scattering is expected to dominate here at low applied field. When H increases, the mixed quadrupolar-magnetic susceptibility becomes nonzero below T_N , and magnetic and quadrupolar excitations can no longer be separated [Fig. 1(d)]. In this case, both magnetic and quadrupole scattering are expected to contribute sizably to the resistivity, with an energy scale set again by Δ_{12} . Indeed, fitting the measured $\rho(T)$ for $T \rightarrow 0$ (Ref. 26) yields an exciton-type contribution with a gap Δ whose value at $H=0$ compares well with the value of Δ_{12} at $T=0$. Also, the calculated $\Delta_{12}(H)$ correlates well with the measured $\Delta(H)$ (see Fig. 2).

Two other peculiar features characterize the measured ρ .²⁶ First, the magnetoresistivity $\Delta\rho(H)$ is positive for $T > 17.5$ K (below 17.5 K it may be nonmonotonic in H , and with both signs, due to the contribution of the anomaly associated with the phase transition, which shifts with H). That $\Delta\rho(H) > 0$ in the paramagnetic phase is unusual since disorder is usually quenched by a magnetic field. More precisely, this is expected to hold in the case of magnetic metals or metals containing magnetic ions, because magnetic scattering decreases with the field. For instance, $\Delta\rho(H) < 0$ for the Kondo, Coqblin-Schrieffer and Anderson models,³⁰ for the two-channel Kondo model,³¹ for heavy-fermion-type models,³² for models based on scattering by paramagnons,³³ or for CEF models based on two low-lying singlets (such as the model used in Ref. 12 to fit the neutron inelastic spectrum) or on a doublet ground state. On the other hand, a positive contribution to the magnetoresistivity is expected in a lattice-periodic Fermi liquid because of the cyclotron motion of conduction electrons.³⁴

So, in magnetic metals and heavy-fermion compounds, the sign of the total magnetoresistivity may change from negative to positive when the temperature is lowered, if the cyclotron contribution begins to exceed the spin fluctuation contribution. However, this positive $\Delta\rho(H)$ is usually observed in the low-temperature range, typically below 10 K in transition-metal compounds [such as ZrZn₂ (Ref. 35) or MnSi (Ref. 36)], and below 1 K in heavy-fermion com-

pounds [such as UBe_{13} ,³⁷ CeAl_3 ,³⁸ CeCu_2Si_2 ,³⁹ or CeCu_6 (Ref. 40)], with the exception, however, of UPt_3 , for which the change of sign takes place somewhere between 4 and 20 K,⁴¹ and of CeRu_2Si_2 , which, up to about 50 K and at low field has a positive magnetoresistivity, which passes through a maximum at $H \sim 8$ T (where a Mott transition of f electrons from itinerant to localized occurs), and becomes negative for $H \geq 12$ T.⁴²

In URu_2Si_2 , the magnetoresistivity is still positive for T as high as 25 K (and monotonically increasing for fields as high as 25 T), and it does not appear to be nearing a change of sign.²⁶ So, it seems unlikely that this positive value be due to cyclotron orbital effects. However, one cannot rule out *a priori* a scenario similar to that of CeRu_2Si_2 , with H driving a localization of f electrons, seen by a positive magnetoresistivity.

In any case, invoking these effects is unnecessary within the present model, since it correctly yields a *positive* magnetoresistivity²⁹ in all (magnetic and quadrupolar) scattering channels. The mechanism is simple: since the gap Δ_{12} diminishes with H [Fig. 1(b)], elastic scattering from static thermal disorder of the O_2^0 quadrupole moments increases with H because of an increased thermal population of the first excited singlet. Also, with a lower Δ_{12} the importance of inelastic scattering processes involving J_z and Q increases (the former processes involve transitions between the two excited singlets).

A second peculiar feature is that although T_N decreases with H , the anomalies observed at T_N do not, and they even increase. The model correctly yields *increasing* OP and anomalies in spite of a decreasing $T_N(H)$. The value of $\langle Q \rangle(T=0, H)$ is given in Fig. 2, and compared with the height of the anomaly measured in ρ . Within the present model, this anomaly is to be attributed to a decrease in the density of states at the Fermi level. This presumably follows a folding of the Brillouin zone due to a modulation of $\langle Q \rangle$, which would yield an increase of the resistivity by a factor proportional to $\langle Q \rangle$ to leading order.⁴³ Another indication of a reconstruction of the Fermi surface taking place at T_N is given by the effective carrier concentration estimated by Hall-effect measurements,⁴⁴ which decreases by about a factor of 10 across T_N . The above scenario is also in agreement with the measured low- T magnetoresistivity near 40 T,⁴⁵ where it displays an abrupt decrease by an amount comparable with the height of the anomaly at T_N , and which is reminiscent of the decrease of $\langle Q \rangle$ evident in Fig. 2.

C. Thermal expansion

The thermal expansion also shows anomalies at $T_N(H)$ whose size strongly increases with H (Ref. 46) (see Fig. 3). The thermal expansion coefficients $(1/a)(da/dT)$ and $(1/c)(dc/dT)$ are proportional to $d\langle O_2^0 \rangle/dT$ through two independent magnetoelastic coefficients.⁴⁷ Since $\langle O_2^0 \rangle$ is a totally symmetric secondary OP, near T_N $d\langle O_2^0 \rangle/dT \propto (d\langle Q \rangle^2/dT + \text{background terms})$.⁴⁸ So, while the height of the anomaly in ρ approximately reflects the value of the OP, the jump in the thermal expansion probes the rate of growth of the OP near T_N . As can be seen in Fig. 3, this rate increases with H , in agreement with experiment.

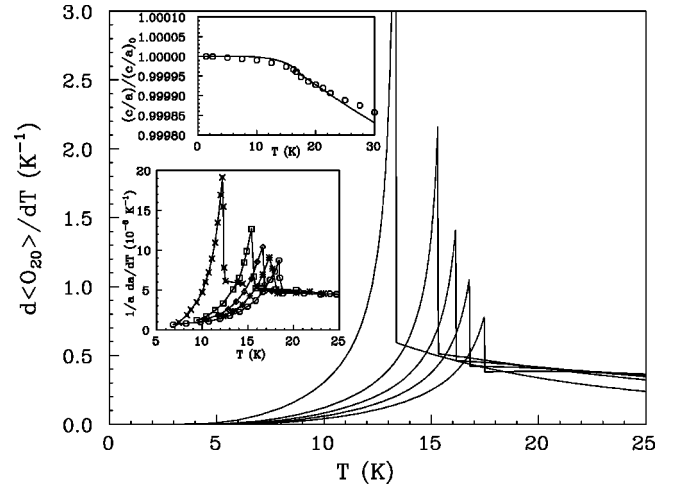


FIG. 3. Temperature derivative of $\langle O_2^0 \rangle$ vs T from (1), with $\lambda = 0.175$ meV. The five curves correspond to $H = 0, 10, 14, 18,$ and 25 T in order of decreasing T_N . Lower inset: measured thermal expansion along a for the same values of H (Ref. 46). The lines are a guide to the eye. Upper inset: calculated normalized c/a ratio vs T . Circles: experiment (Ref. 49).

The calculated c/a ratio vs T for $H = 0$ is compared with experiment⁴⁹ in the inset. The c/a ratio is roughly proportional to $\langle O_2^0 \rangle$. This quantity indicates in fact whether the charge distribution on U ions is prolate or oblate with respect to the c axis. In particular, since the coefficient relating the quadrupole moment $Q_2^0 = \sum_i [3z_i^2 - r_i^2]$ within the 3H_4 multiplet to its equivalent operator $O_2^0(\mathbf{J})$ is negative, a negative $\langle O_2^0 \rangle$ means a prolate charge distribution and an increase of the c/a ratio is expected as $\langle O_2^0 \rangle$ decreases. The increase of c/a on cooling and the change in slope at T_N are well reproduced.

In the above discussion the thermal expansion was entirely attributed to the magnetoelastic coupling of the lattice to the T -dependent quadrupolar moment of U ions. The pure lattice contribution to the thermal expansion was omitted. In fact, anharmonic lattice effects can usually be neglected below ~ 20 K in intermetallic compounds.⁵⁰ Measurements of the thermal expansion of the homologous non- f compound ThRu_2Si_2 (Ref. 51) indeed indicate that the lattice contribution is small for $T \leq 20$ – 30 K. The contribution of the OP to the thermal expansion was neglected too, since for antiferro-quadrupolar ordering the effect on uniform lattice properties is expected to be small.

D. Magnetization for weak magnetic exchange

The model is compatible with the observed metamagnetic transitions at $H \sim 35$ – 40 T.⁴⁵ Multistep metamagnetic transitions in f -electron compounds are usually thought to be the result of competing exchange interactions,⁵² with a zero-field state of AFM type. By applying an external field the magnetization increases in discontinuous steps, corresponding to a reversal of some of the spins. Eventually, the fully polarized state, having all moments pointing in the direction of the field, is produced. In Ref. 45 a model of this type is proposed for URu_2Si_2 . It is assumed that U ions carry a pseudospin $S = \frac{1}{2}$, to which is associated a moment $gS = 1\mu_B$. These

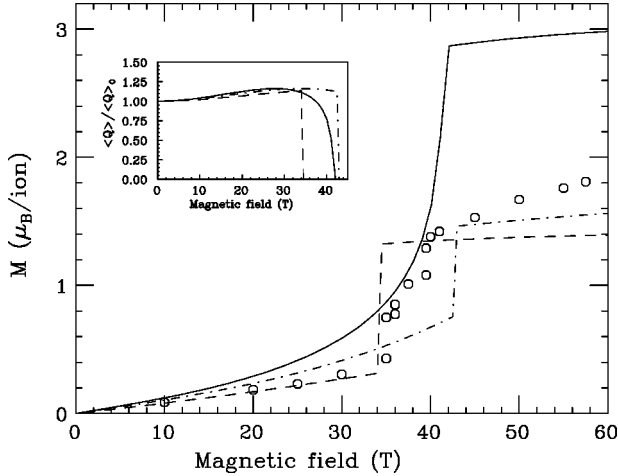


FIG. 4. Magnetization M at $T=0$ vs field from the two-sublattice mean-field approximation of Eq. (3). Inset: staggered order parameter. Full lines: $J_Q=0.022$ meV, $J_M=0$, and $J_1=0$ [corresponding to Eq. (1) with $\lambda=0.175$ meV]. Dash-dotted lines: $J_Q=0.022$ meV, $J_M=0.056$ meV, and $J_1=0$. Dashed lines: $J_Q=0.022$ meV, $J_M=0.178$ meV, and $J_1=0.037$ meV. $\langle Q \rangle_0=3.76$ for the three sets. Circles: experiment (Ref. 45).

spins interact through first-, second-, and third-nearest-neighbor exchange interactions. The free energy for various spin configurations is calculated in mean field. By properly choosing the strength of the exchange interactions, the lowest-energy spin configuration in zero external field is an antiferromagnetic state of the type observed in URu₂Si₂. When an external field is applied, this state evolves into a ferromagnetic state through three metamagnetic transitions, in which some of the spins are reversed. As usual with models assuming only AFM order to occur in URu₂Si₂, one has the problem that an AFM order much stronger than observed is necessary to explain the macroscopic behavior. Indeed, the staggered moment of the zero-field state is gS , much larger than the observed moment of $0.03\mu_B$.

In the present model, the U ions in zero field have no average magnetic moment. The microscopic process at the basis of the metamagnetic transition is not a spin reversal but rather a crossing of levels, which occurs in the single-ion CEF Hamiltonian at a critical field $H_c \sim 37$ T [corresponding to $\Delta_{12}(H_c)=0$]. For the single-ion CEF Hamiltonian [i.e., Eq. (1) with $\lambda=0$], at $T=0$ the moment jumps from about $0.3\mu_B$ for $H < H_c$ to about $2.8\mu_B$ for $H > H_c$. By taking into account the quadrupolar ordering ($\lambda \neq 0$), the crossing becomes an anticrossing and the transition is smeared (full line in Fig. 4).

In a lattice of U ions, the transition can acquire a multi-step character as a result of magnetic exchange interactions. That such interactions exist, and are of AFM type, is demonstrated by the strong dispersion observed in the magnetic excitations, with a minimum at the wave vector of the tiny-moment AFM state,¹² and by the negative Curie-Weiss constant λ_0 translating the inverse uniform susceptibility.⁹

Because of the AFM character of exchange interactions, there is competition between CEF and Zeeman interactions on the one hand (these would favor a high-moment state on all U ions for $H > H_c$), and exchange interactions on the other (for these latter a high-moment ferromagnetic state is

costly). This competition is resolved by a compromise, i.e., only some of the U ions undergo the level crossing at H_c . Above H_c there are intermediate phases with inhomogeneous magnetization. This effect cannot be studied within model (1), which is a one-sublattice model, and a multisublattice calculation is necessary.

The minimal model is a two-sublattice model, with one sublattice representing the corners, and the other the center of the body-centered-tetragonal cell. This implies choosing for the unknown ordering wave vector \vec{K}_Q , giving the modulation of the sign of $\langle Q \rangle$, either zero (ferroquadrupolar structure) or the same value as for the tiny-moment AFM state, with $\langle Q \rangle$ having opposite signs on the two sublattices. The same results are obtained with the two choices of \vec{K}_Q .

To minimize the number of parameters, only couplings between nearest neighbors on different sublattices are considered. The Hamiltonian is

$$\mathcal{H} = \sum_i \sum_{k,q} B_k^q O_k^q(i) + J_Q \sum_{i \in 1, j \in 2} Q(i)Q(j) + J_M \sum_{i \in 1, j \in 2} J_z(i)J_z(j) - \sum_i g\mu_B J_z(i)H. \quad (2)$$

Making the MF approximation in Eq. (2) and allowing for two sublattices leads to two effective single-ion Hamiltonians, with four linked self-consistency conditions for $\langle Q \rangle_1$, $\langle Q \rangle_2$, $\langle J_z \rangle_1$, and $\langle J_z \rangle_2$ to be imposed. This is equivalent to minimizing the corresponding MF free energy $\mathcal{F}_{\text{MF}}(\langle Q \rangle_1, \langle Q \rangle_2, \langle J_z \rangle_1, \langle J_z \rangle_2)$, as given by the Bogolyubov variational principle.⁵³

If $J_M=0$, the state minimizing \mathcal{F}_{MF} has $|\langle Q \rangle_1| = |\langle Q \rangle_2|$, and $\langle J_z \rangle_1 = \langle J_z \rangle_2$. In this case, Eq. (2) is equivalent to Eq. (1), with J_Q related to the molecular field constant λ appearing in Eq. (1) by $J_Q = \pm \lambda/8 = \pm 0.022$ meV (only the model giving $T_N=17.5$ K will be considered in the following). The positive and negative sign correspond to antiferroquadrupolar and ferroquadrupolar ordering, respectively. If $J_M \neq 0$, $|\langle Q \rangle_1| = |\langle Q \rangle_2|$ and $\langle J_z \rangle_1 = \langle J_z \rangle_2$ only for $H < H_c$, while above H_c the state which minimizes \mathcal{F}_{MF} does not have the same magnetization on the two sublattices.

The actual value of J_M can be related to the Curie-Weiss constant $\lambda_0 \propto J_M$ translating the inverse uniform susceptibility. The value $\lambda_0 \sim -69$ mole/emu, which was estimated in Ref. 9, gives a positive (antiferromagnetic) $J_M \sim 0.18$ meV. With this choice of J_M one has the correct value of the susceptibility, i.e., the correct slope of the magnetization $M = g\mu_B(\langle J_z \rangle_1 + \langle J_z \rangle_2)$ at low fields.

We would like now to comment about the type of interion couplings considered in Eq. (2). In principle, at the MF level one should consider interion couplings in the calculation for all those multipoles whose expectation value is non-zero. Thus, beyond the interion couplings involving J_z and Q , one should also consider couplings involving symmetric electric multipoles (the O_k^q appearing in the CEF Hamiltonian). Interion interactions involving these multipoles are expected to originate from the mechanism (whichever it is) producing the coupling J_Q in Eq. (2), and to be of the same

order of magnitude as J_Q . Couplings involving J_x or J_y , as well as nonsymmetric multipoles belonging to a representation different from that of Q or J_z , do not play any role at the MF level, since their expectation value is zero for any value of the field. In principle, couplings involving high rank (≥ 3) magnetic multipoles belonging to the same representation as J_z (Γ_{12}) as well as high rank (≥ 4) electric multipoles belonging to the same representation as Q (Γ_{13} or Γ_{14}) should also be considered. These latter should also have been considered in Eq. (1). However, to a great extent these high-order couplings may be taken into account implicitly through a renormalization of the coupling constants for the corresponding low-rank multipoles. They will therefore be neglected to avoid proliferation of parameters, and because the level of the calculation is only intended to be semiquantitative. To minimize the number of parameters, we also neglect for the moment couplings involving the O_k^q , although these are not expected to be small.

Only $T=0$ is considered, and \mathcal{F}_{MF} is minimized with respect to the four variational parameters by the simplex method. The equivalence of Eqs. (1) and (2) for $J_M=0$ is seen by comparing the staggered OP $\langle Q \rangle = (\langle Q \rangle_1 - \langle Q \rangle_2)/2$ (Fig. 4), with $\langle Q \rangle$ calculated from (1) (Fig. 2).

The magnetization for $J_M=0$ is shown in Fig. 4. Above the metamagnetic transition it is about twice as large as the measured one. However, if $J_M > 0$ the transition occurs in two steps, since one sublattice undergoes the transition at $H_1 \sim 35\text{--}40$ T, and the other at $H_2 > H_1$, with $H_2 - H_1$ increasing with increasing J_M . For instance, the dash-dotted line in Fig. 4 corresponds to $J_M = 0.056$ meV. This low value of J_M gives already a high $H_2 \sim 75$ T, above the maximum field used in the experiment.

It must be stressed that we are not trying to reproduce the three-step structure of the transition observed for H between 35 and 40 T, which within our two-sublattice model collapse in the single transition occurring at H_1 .

E. Magnetization for strong magnetic exchange

For $J_M \geq 0.11$ meV, there is a problem with model (2), since the zero-field quadrupolar state becomes metastable, and a Blume-type⁵⁴ first-order transition towards an AFM state with $\mu \sim 3\mu_B$ takes place, with the moments pointing in opposite directions on the two sublattices (the wave vector \vec{K} of this AFM state would be the same as for the tiny-moment state). The parameter controlling this transition is the value $J_M(\vec{K})$ of the Fourier-transformed exchange couplings at \vec{K} . On the other hand, the Curie-Weiss constant λ_0 used above to fix the value of J_M is proportional to $J_M(0)$. Since, within Eq. (2), $J_M(\vec{K}) = -J_M(0)$, one cannot reduce the value of $J_M(\vec{K})$, and eliminate in this way the instability, without worsening the comparison with the susceptibility. A possibility is to introduce intrasublattice exchange, with coupling constant J_M^1 , in addition to intersublattice exchange, with coupling constant J_M^2 . In this way one decouples $J_M(\vec{K})$ and $J_M(0)$, since $J_M(0) \propto J_M^1 + J_M^2$, while $J_M(\vec{K}) \propto J_M^1 - J_M^2$. So, by properly choosing J_M^1 and J_M^2 one can reduce the value of $J_M(\vec{K})$ enough to eliminate the instability, with no effect on the susceptibility.

We do not find the scenario outlined above satisfying. In fact, the parameter $J_M(\vec{K})$ also controls the energy of magnetic excitations with wave vector \vec{K} . The fact that these excitations are particularly soft,¹² suggests that $J_M(\vec{K})$ is not small, or at least not small enough for the instability to be eliminated.

It must be stressed that this type of instability is not related to the specific form of model (2) nor to the type of OP proposed. For high enough $J_M(\vec{K})$ it would be found in any model based on local degrees of freedom in a molecular field, whose nonlinear susceptibility is positive and whose linear susceptibility decreases with decreasing T , as observed in URu_2Si_2 .

We show in the following that even if $J_M(\vec{K})$ is not small, a mechanism removing the high-moment AFM state may be found in the couplings involving symmetric electric multipoles, the O_k^q , which were neglected in Eq. (2). These interactions may compete with exchange by raising the energy of the high-moment AFM state. For instance, since the high-moment AFM state induces a strong *uniform* increase of $\langle O_2^0 \rangle$, antiferroquadrupolar couplings involving the axial quadrupolar moment O_2^0 would disfavor the AFM state. In other words, there is one (or more) secondary OP associated with the staggered moment, for which the high-moment AFM state is costly in energy.

In the following we consider Hamiltonian (2), to which a coupling involving the O_k^q and raising the energy of the high-moment AFM state is added:

$$\mathcal{H} = \mathcal{H}_0 + J_1 \sum_{i \in 1, j \in 2} O(i)O(j), \quad (3)$$

where \mathcal{H}_0 is given by Eq. (2), and O is a symmetric multipole (i.e., one or a linear combination of the O_k^q) whose average value is higher in the high-moment AFM state than in the paramagnetic or quadrupolar-ordered state. In this way, if $J_1 > 0$ the new coupling tends to make the AFM state less favorable (a Landau-type formulation of this situation is given in the Appendix).

As said above, O_2^0 might be a good candidate for O . Unfortunately, studying the MF problem with six coupled self-consistent fields is difficult. Just to illustrate how this interaction may work, we study the MF problem without imposing self-consistency on $\mathcal{H}_1 = J_1 \sum_{i \in 1, j \in 2} O(i)O(j)$, i.e., by keeping the same four variational parameters as with Eq. (2), with \mathcal{H}_1 acting only as an energy shift. To minimize the error, O is chosen so that loss of self-consistency is minimal, and even zero for $H=0$: $O = (J^2)|3\rangle\langle 3|$, with $|3\rangle$ the second excited state of the CEF Hamiltonian [Γ_{12} ; see Fig. 1(a)]. This operator corresponds to the projection onto the three low-lying singlets of a suitable linear combination of O_2^0 , O_4^0 , and O_6^0 . Loss of self-consistency is minimal with this choice of O because the weight of state $|3\rangle$ in the MF ground state tends to zero for small values of the applied field.

Choosing $J_1 \geq 0.03$ meV removes the first-order transition, and (in view of the approximations made) gives a reasonably good description of the magnetization (see Fig. 4). Loss of self-consistency is appreciable only above the metamagnetic transition, where the calculated $M(H)$ is only

qualitative. Note that J_1 is of order $\mathcal{O}(J_Q)$, which is expected if the origin of J_1 and J_Q is common.

Models (2) and (3) treated in a MF approximation using more than two sublattices are expected to yield a multistep transition in the region around 40 T if a suitable choice of the exchange couplings is made, as in Ref. 45. This expectation is supported by calculations we made for finite clusters of U ions with various geometries. The exact ground state for Hamiltonians analogous to Eqs. (2) or (3) can be calculated by the Lanczos method⁵⁵ for clusters containing 6–8 sites. The magnetization is found to possess multistep transitions when the exchange couplings introduce frustration.

Putting $J_M, J_1 \neq 0$ is not expected to affect appreciably the quantities calculated above with Eq. (1) (see, for instance, the staggered OP in Fig. 4). In fact, the effect of J_M and J_1 is qualitatively important only for high values of the field, above the metamagnetic transition.

III. INELASTIC NEUTRON SCATTERING IN AN APPLIED FIELD

The peculiar behavior of URu₂Si₂ in a magnetic field discussed in this paper originates from the existence of two distinct energy scales Δ_{12} and Δ_{13} . For $T < T_N$, if $H = 0$ only Δ_{13} can be probed by INS, while for finite H they should *both* be seen. In this case, in fact, a nonzero matrix element of J_z between $|1\rangle$ and $|2\rangle$ exists [Fig. 1(d)].

If the dispersion of excitations is neglected, the oscillator strength is $|\langle 1 | J_z | 2 \rangle|^2 = 0$ for $H = 0$, $\sim 10^{-2} |\langle 1 | J_z | 3 \rangle|^2$ for $H \sim 3$ T, $\sim 0.2 |\langle 1 | J_z | 3 \rangle|^2$ for $H \sim 14$ T. Thus it would be interesting to perform INS in a field of the order of 15 T along c to see directly whether this second energy scale actually exists. This would also be interesting in relation to the OP proposed in Ref. 19, i.e., $Q_{xy}Q_{x^2-y^2}$, an electric multipole of rank 4 belonging to representation Γ_{12} . This representation is the same as that to which J_z belongs, but the properties of the two multipoles under time reversal are opposite.

The molecular field associated with this OP would presumably mix a ground CEF singlet $|\Gamma_{11}\rangle$ with $|\Gamma_{12}\rangle$, since $\Gamma_{12} = \Gamma_{11} \times \Gamma_{12}$ (see also Ref. 9, where this model is called ‘‘scheme A’’). The only remaining possibility is that ground and excited CEF singlets belong to Γ_{13} and Γ_{14} , since $\Gamma_{12} = \Gamma_{13} \times \Gamma_{14}$. However, this second possibility seems unlikely. In fact, the matrix element $\langle \Gamma_{13} | g\mu_B J_z | \Gamma_{14} \rangle = 1.6\mu_B$ for any choice of the CEF parameters. Because J_z is odd under time reversal, this value remains the same (in modulus) if the two singlets are mixed by the time-even molecular field. However, the measured value of the matrix element of J_z is $1.2\mu_B$ in zero applied magnetic field.¹² This value can only be reproduced with $|\Gamma_{11}\rangle$ and $|\Gamma_{12}\rangle$ low-lying states, since $\langle \Gamma_{11} | g\mu_B J_z | \Gamma_{12} \rangle$ may range from zero to $3.2\mu_B$ when CEF parameters vary.

Although it is possible in principle that the value of $\langle \Gamma_{13} | g\mu_B J_z | \Gamma_{14} \rangle$ be smaller than $1.6\mu_B$ due to corrections to the Russel-Saunders coupling scheme (such as J -mixing effects or orbital reduction factors), one could not explain the fact that the magnetization in an applied field reaches $\sim 2\mu_B$ at 60 T (see Fig. 4). In fact, with Γ_{13} and Γ_{14} low-lying states the magnetization would saturate to $\langle \Gamma_{13} | g\mu_B J_z | \Gamma_{14} \rangle$. On the

other hand, with Γ_{11} and Γ_{12} low-lying states there is not this problem, since the magnetization would saturate to $3.2\mu_B$.

If $H = 0$, the INS experiment would detect the transition between the two singlets ($|1'\rangle$ and $|2'\rangle$) resulting from the mixing of $|\Gamma_{11}\rangle$ and $|\Gamma_{12}\rangle$ by the electric-multipole molecular field. Unless the localized picture is completely wrong (which does not seem to be the case, at least below T_N), it can be shown that this model necessarily leads to the presence of a third singlet $|3'\rangle$ ($\equiv |\Gamma_{11}^2\rangle$ above T_N) a few meV above $|2'\rangle$.⁵⁶ This is estimated from the gap $E(2') - E(1') \sim 10$ meV and from the matrix element $\langle 1' | g\mu_B J_z | 2' \rangle = 1.2\mu_B$ measured in INS.¹²

By applying a magnetic field, the third singlet would also become visible by INS. Our estimates for the oscillator strengths are $|\langle 1' | J_z | 3' \rangle|^2 = 0$ for $H = 0$, $\sim 0.1 |\langle 1' | J_z | 2' \rangle|^2$ for $H \sim 3$ T, and $\sim 0.2 |\langle 1' | J_z | 2' \rangle|^2$ for $H \sim 14$ T. Therefore this second energy scale should be seen by making INS in an applied field even more easily than Δ_{12} .

In all the above estimations of oscillator strengths, dispersion has been neglected. Since in reality both gaps and oscillator strengths are wave vector dependent, these estimations are merely to be taken as order of magnitudes. Measuring at a wave vector not too close to the zone center or to the zone boundaries should make dispersion effects lower.

IV. CONCLUSIONS

The compound URu₂Si₂ displays a number of peculiar properties, which are difficult to understand, even qualitatively, on the basis of a heavy-fermion or Kondo-lattice-type of picture. While such a picture is probably appropriate for UPt₃, where a tiny-moment state similar to that of URu₂Si₂ is observed, the macroscopic behavior of the two compounds is profoundly different. In Ref. 9 it was shown that a model based on quadrupolar ordering of localized f electrons is able to reproduce the macroscopic behavior of URu₂Si₂ in zero or infinitesimal applied magnetic field at a semiquantitative level. In particular, the model can explain why the magnetic susceptibility χ is strongly anisotropic, and $\chi(T)$ has a pronounced maximum around $T \sim 50$ K for a field applied along the c axis. It can also explain the specific heat maximum at $T \sim 30$ K; the value of the transition temperature; the value of the oscillator strength of magnetic excitations measured by INS, and the polarization along c of these excitations; the value of the entropy at T_N ; that the susceptibility for a field applied along the c axis has a discontinuous increase of the slope in lowering the temperature through T_N ; that the nonlinear susceptibility has an unusual λ -type anomaly at T_N ; that the $(C_{11} - C_{12})$ elastic constant softens below $T \sim 70$ K (Ref. 21); and the point-contact spectroscopy results.²⁰

In the present paper, the behavior of URu₂Si₂ in a finite applied magnetic field along the c axis has been analyzed. Experiments have shown that the transition temperature as determined by macroscopic anomalies decreases with the field, and reduces to zero at a field close to 40 T; that the resistivity contains a contribution due to scattering from localized excitations, whose energy scale decreases with the field similarly to the transition temperature; that the magnetoresistivity is positive above T_N ; that the anomaly in the

resistivity at T_N increases slightly with increasing field; that the anomaly in the thermal expansion increases strongly with increasing field; that the zero-field c/a ratio increases with decreasing temperature above T_N , and it has a discontinuous increase of the slope at T_N ; and that there are metamagnetic transitions for a field between 35 and 40 T, with the magnetization passing from about $0.4\mu_B$ to $1.4\mu_B$. It has been shown that all these properties may be understood in the framework of the model. It is clear that since none of the observables considered probes the antiferroquadrupolar OP directly, but only through its effect on other (measurable) quantities, there is still in principle the possibility that the agreement obtained is fortuitous, and that the OP be different than supposed. The proposed INS experiment in a high field should enable a further test of the model to be made.

ACKNOWLEDGMENTS

The author acknowledges helpful discussions with G. Amoretti, P. Erdős, and P. Thalmeier, and the support of the Swiss National Science Foundation through Grant No. 20-046686.96/1.

APPENDIX

A qualitative Landau-type model for the free energy of Eqs. (2) and (3) is given in the following. We neglect for simplicity the quadrupolar OP Q and the external field, i.e., we consider the case $J_Q=0$, $H=0$. In fact these do not affect qualitatively the AFM instability, on which we focus here. Calling μ the staggered moment ($\langle J_z \rangle_1 - \langle J_z \rangle_2$), and ζ the symmetric secondary OP ($\langle O \rangle_1 + \langle O \rangle_2$), a minimal Landau-type model for the MF free energy of Eqs. (2) and (3) is

$$\mathcal{F}_L = \frac{a(T-T_C)}{2} \mu^2 + \frac{b}{4} \mu^4 + \frac{c}{6} \mu^6 + d(\zeta - \zeta_0)^2 + e\mu^2(\zeta - \zeta_0) + f\mu^2(\zeta - \zeta_0)^2, \quad (\text{A1})$$

with $a>0$, $d>0$, and $f>0$. If $\mu=0$ one has $\zeta=\zeta_0$, the ‘background’ value of the secondary OP [actually in the

literature it is sometimes $(\zeta - \zeta_0)$ which is called secondary OP].

Minimizing \mathcal{F}_L with respect to ζ one gets an effective free energy for μ of the form

$$\mathcal{F}_L = \frac{a(T-T_C)}{2} \mu^2 + \frac{\tilde{b}}{4} \mu^4 + \frac{\tilde{c}}{6} \mu^6, \quad (\text{A2})$$

with renormalized parameters $\tilde{b}=b-e^2/d$ and $\tilde{c}=c+3e^2f/(2d^2)$.

Model (2) in the mean field approximation is qualitatively similar to Eqs. (A1) and (A2), with $\tilde{b}<0$ and $\tilde{c}>0$, which for μ gives a standard Landau-type model for a first-order phase transition. More precisely, for $T>T_2=T_C + \tilde{b}^2/(4\tilde{c}a)$ the phase with $\mu=0$ is stable, for $T_2>T>T_1 = T_C + 3\tilde{b}^2/(16\tilde{c}a)$, the phase with $\mu=0$ is stable, but a metastable phase with $\mu \neq 0$ appears; for $T_1>T>T_C$ the phase with $\mu \neq 0$ is stable, but the phase with $\mu=0$ remains metastable; and for $T<T_C$, only the stable phase with $\mu \neq 0$ remains.

For $J_M \leq 0.11$ meV, model (2) corresponds to Eq. (A2) with $T_C, T_1 < 0$. At $T=0$ the stable state is paramagnetic (or quadrupolar for the assumed nonzero J_Q), and the AFM state is metastable (or even unstable for $J_M \rightarrow 0$). The case $J_M \geq 0.11$ meV corresponds to the situation when $T_C < 0$ and $T_1 > 0$. At $T=0$ the AFM state is stable, with a metastable paramagnetic (or quadrupolar) state. Only for $J_M \geq 0.35$ meV one has $T_C > 0$ and does the metastable paramagnetic state disappear.

Introducing the coupling J_1 in Eq. (3) is analogous to modifying the values of d, e, f , and ζ_0 in Eq. (A1). Note that the modification of ζ_0 may be seen effectively as a renormalization of the CEF parameters B_k^q . The elimination of the first-order transition toward the AFM state may be understood as due to an increase of f . This leads to an increase of \tilde{c} which makes T_1 negative. All the above is only qualitative because the high value of μ and $\zeta - \zeta_0$ in the AFM state is expected to make higher-order terms in \mathcal{F}_L important.

¹K. A. Gschneider, Jr., J. Tang, S. K. Dhar, and A. Goldman, *Physica B* **163**, 507 (1990).

²C. L. Lin, A. Wallash, J. E. Crow, T. Mihalisin, and A. Goldman, *Phys. Rev. Lett.* **58**, 1232 (1987).

³R. M. White and P. Fulde, *Phys. Rev. Lett.* **47**, 1540 (1981).

⁴J. M. Fournier, A. Blaise, G. Amoretti, R. Caciuffo, J. Larroque, M. T. Hutchings, R. Osborn, and A. D. Taylor, *Phys. Rev. B* **43**, 1142 (1991).

⁵B. Hålg and A. Furrer, *Phys. Rev. B* **34**, 6258 (1986).

⁶R. Osborn, M. Hagen, D. L. Jones, W. G. Stirling, G. H. Lander, K. Mattenberger, and O. Vogt, *J. Magn. Magn. Mater.* **76-77**, 429 (1988).

⁷C. Bergemann, S. R. Julian, G. J. McMullan, B. K. Howard, G. G. Lonzarich, P. Lejay, J. P. Brison, and J. Floquet, *Physica B* **230-232**, 348 (1997).

⁸G. J. Rozing, P. E. Mijnders, and D. D. Koelling, *Phys. Rev. B* **43**, 9515 (1991); G. J. Rozing, P. E. Mijnders, A. A. Men-

ovsky, and P. F. de Châtel, *ibid.* **43**, 9523 (1991).

⁹P. Santini and G. Amoretti, *Phys. Rev. Lett.* **73**, 1027 (1994).

¹⁰R. S. Craig, S. G. Sankar, N. Marzouk, V. U. S. Rao, W. E. Wallace, and E. Segal, *J. Phys. Chem. Solids* **33**, 2267 (1972).

¹¹V. M. T. S. Barthem, D. Gignoux, A. Nait-Saada, D. Schmitt, and G. Creuzet, *Phys. Rev. B* **37**, 1733 (1988).

¹²C. Broholm, J. K. Kjems, W. J. L. Buyers, P. Matthews, T. T. M. Palstra, A. A. Menovsky, and J. A. Mydosh, *Phys. Rev. Lett.* **58**, 1467 (1987); C. Broholm, H. Lin, P. Matthews, T. E. Mason, W. J. L. Buyers, M. F. Collins, A. A. Menovsky, J. A. Mydosh, and J. K. Kjems, *Phys. Rev. B* **43**, 12 809 (1991).

¹³J. P. Brison, N. Keller, P. Lejay, A. Huxley, L. Schmidt, A. Buzdin, N. R. Bernhoeft, I. Mineev, A. N. Stepanov, J. Flouquet, D. Jaccard, S. R. Julian, and G. G. Lonzarich, *Physica B* **199-200**, 70 (1994); G. Oomi, T. Kagayama, Y. Onuki, and T. Komatsubara, *ibid.* **199-200**, 148 (1994).

¹⁴S. Doniach, in *Valence Instabilities and Related Narrow-Band*

- Phenomena*, edited by R. D. Parks (Plenum, New York, 1977).
- ¹⁵E. D. Isaacs, D. B. McWhan, R. N. Kleiman, D. J. Bishop, G. E. Ice, P. Zschack, B. D. Gaulin, T. E. Mason, J. D. Garrett, and W. J. L. Buyers, *Phys. Rev. Lett.* **65**, 3185 (1990); T. E. Mason, B. D. Gaulin, J. D. Garrett, Z. Tun, W. J. L. Buyers, and E. D. Isaacs, *ibid.* **65**, 3189 (1990); M. B. Walker, W. J. L. Buyers, Z. Tun, W. Que, A. A. Menovsky, and J. D. Garrett, *ibid.* **71**, 2630 (1993).
- ¹⁶B. Fåk, C. Vettier, J. Flouquet, F. Bourdarot, S. Reymond, A. Vernière, P. Lejay, Ph. Boutrouille, N. R. Bernhoeft, S. T. Bramwell, R. A. Fisher, and N. E. Phillips, *J. Magn. Magn. Mater.* **154**, 339 (1996).
- ¹⁷L. P. Gor'kov, *Europhys. Lett.* **16**, 301 (1991).
- ¹⁸A. P. Ramirez, P. Coleman, P. Chandra, E. Brück, A. A. Menovsky, Z. Fisk, and E. Bucher, *Phys. Rev. Lett.* **68**, 2680 (1992).
- ¹⁹V. Barzykin and L. P. Gor'kov, *Phys. Rev. Lett.* **74**, 4301 (1995).
- ²⁰J. G. Rodrigo, F. Guinea, S. Vieira, and F. G. Aliev, *Phys. Rev. B* **55**, 14 318 (1997).
- ²¹K. Kuwahara, H. Amitsuka, T. Sakakibara, O. Suzuki, S. Nakamura, T. Goto, M. Mihalik, A. A. Menovsky, A. de Visser, and J. J. M. Franse, *J. Phys. Soc. Jpn.* **66**, 3251 (1997).
- ²²M. B. Walker and W. J. L. Buyers, *Phys. Rev. Lett.* **74**, 4097 (1995); P. Santini and G. Amoretti, *ibid.* **74**, 4098 (1995).
- ²³J. M. Effantin, J. Rossat-Mignod, P. Burlet, H. Bartholin, S. Kunnii, and T. Kasuya, *J. Magn. Magn. Mater.* **47-48**, 145 (1985).
- ²⁴P. Morin and D. Schmitt, in *Ferromagnetic Materials*, edited by K. H. J. Buschow and E. P. Wohlfarth (Elsevier, Amsterdam, 1990).
- ²⁵D. J. Allen, *Phys. Rev.* **166**, 530 (1968); **167**, 492 (1968).
- ²⁶S. A. M. Mentink, T. E. Mason, S. Süllow, G. J. Nieuwenhuys, A. A. Menovsky, J. A. Mydosh, and J. A. A. J. Perenboom, *Phys. Rev. B* **53**, R6014 (1996).
- ²⁷J.-G. Park, K. A. McEwen, S. de Brion, G. Chouteau, H. Amitsuka, and T. Sakakibara, *J. Phys.: Condens. Matter* **9**, 3065 (1997).
- ²⁸The symmetry-breaking quadrupolar moment on site i , $\langle Q(i) \rangle$, is oscillating in sign as $\cos(\vec{K}_Q \cdot \vec{R}_i)$, with \vec{K}_Q the (unknown) ordering wave vector. This wave vector appears in (1) only implicitly through the definition of the molecular field constant λ as the Fourier transform at \vec{K}_Q of the real-space quadrupolar coupling constants. However, to use Eq. (1), $|\langle Q(i) \rangle|$ is assumed to be independent of i (nonmodulated structure). It coincides with $|\langle Q \rangle|$. Note that the symmetric axial quadrupolar moment $\langle O_2^0(i) \rangle$ is independent of i . It is nonzero due to the CEF.
- ²⁹N. Hessel Andersen, in *Crystalline Electric Field and Structural Effects in f-Electron Systems*, edited by J. E. Crow, R. P. Guertin and T. Mihalisin (Plenum, New York, 1980), p. 373 and references therein; N. Hessel Andersen, J. Jensen, H. Smith, O. Splitteroff, and O. Vogt, *Phys. Rev. B* **21**, 189 (1980).
- ³⁰P. Schlottmann, *Phys. Rep.* **181**, 2 (1989).
- ³¹F. B. Anders, M. Jarrell, and D. L. Cox, *Phys. Rev. Lett.* **78**, 2000 (1997).
- ³²S. H. Liu, *Phys. Rev. B* **37**, 3542 (1988).
- ³³P. Hertel, J. Appel, and D. Fay, *Phys. Rev. B* **22**, 534 (1980).
- ³⁴C. Kittel, *Quantum Theory of Solids* (Wiley, New York, 1963).
- ³⁵S. Ogawa, *Physica B* **91**, 82 (1977).
- ³⁶K. Kadowaki, K. Okuda, and M. Date, *J. Phys. Soc. Jpn.* **51**, 2433 (1982).
- ³⁷U. Rauschschwalbe, F. Steglich, and H. Rietschel, *Europhys. Lett.* **1**, 71 (1986).
- ³⁸G. Remeny, A. Briggs, J. Flouquet, O. Laborde, and F. Lapierre, *J. Magn. Magn. Mater.* **31-34**, 407 (1983).
- ³⁹U. Rauchschwalbe, W. Baus, S. Horn, H. Spille, F. Steglich, F. R. de Boer, J. Aarts, W. Assmus, and M. Herrmann, *J. Magn. Magn. Mater.* **47-48**, 33 (1985).
- ⁴⁰Y. Onuki and T. Komatsubara, *J. Magn. Magn. Mater.* **63-64**, 281 (1987).
- ⁴¹A. de Visser, R. Gersdorf, J. J. M. Franse, and A. Menovsky, *J. Magn. Magn. Mater.* **54-57**, 383 (1986).
- ⁴²P. Haen, J. Flouquet, F. Lapierre, P. Lejay, and G. Remenyi, *J. Low Temp. Phys.* **67**, 391 (1987).
- ⁴³H. Miwa, *Prog. Theor. Phys.* **29**, 477 (1963).
- ⁴⁴J. Schoenes, C. Schönenberger, J. J. M. Franses, and A. A. Menovsky, *Phys. Rev. B* **35**, 5375 (1987); A. LeR Dawson, W. R. Datars, J. D. Garrett, and F. S. Razavi, *J. Phys.: Condens. Matter* **1**, 6817 (1989).
- ⁴⁵K. Sugiyama, H. Fuke, K. Kindo, K. Shimohata, A. A. Menovsky, J. A. Mydosh, and M. Date, *J. Phys. Soc. Jpn.* **59**, 3331 (1990).
- ⁴⁶S. A. M. Mentink, U. Wyder, J. A. A. J. Perenboom, A. de Visser, A. A. Menovsky, G. J. Nieuwenhuys, J. A. Mydosh, and T. E. Mason, *Physica B* **230-232**, 74 (1997).
- ⁴⁷P. Morin, J. Rouchy, and D. Schmitt, *Phys. Rev. B* **37**, 5401 (1988).
- ⁴⁸J.-C. Tolédano and P. Tolédano, *The Landau Theory of Phase Transitions* (World Scientific, New York, 1987), p. 20.
- ⁴⁹A. de Visser, F. E. Kayzel, A. A. Menovsky, J. J. M. Franse, J. van den Berg, and G. Nieuwenhuys, *Phys. Rev. B* **34**, 8168 (1986).
- ⁵⁰P. Thalmeier and B. Lüthi, in *Handbook on the Physics and Chemistry of Rare Earths*, edited by K. A. Gschneider, Jr. and L. Eyring (Elsevier, Amsterdam, 1991), Vol. 14.
- ⁵¹H. Amitsuka, T. Sakakibara, A. de Visser, F. E. Kayzel, and J. J. M. Franse, *Physica B* **230-232**, 613 (1997).
- ⁵²H. Fujii and T. Shigeoka, *J. Magn. Magn. Mater.* **90-91**, 115 (1990).
- ⁵³H. B. Callen, *Thermodynamics and an Introduction to Thermostatistics*, 2nd ed. (Wiley, New York, 1985), p. 433.
- ⁵⁴M. Blume, *Phys. Rev.* **141**, 517 (1966).
- ⁵⁵J. K. Cullum and R. A. Willoughby, *Lanczos Algorithms for Large Symmetric Eigenvalue Computations* (Birkhäuser, Boston, 1985).
- ⁵⁶This is because there are constraints in the $|\Gamma_{t1}^1\rangle - |\Gamma_{t2}\rangle - |\Gamma_{t1}^2\rangle$ subspace [see G. Amoretti, A. Blaise, and J. Mulak, *J. Magn. Magn. Mater.* **42**, 65 (1984)], which persist in the presence of an electric multipole molecular field belonging to Γ_{t2} .